Journal of Autoimmunity 133 (2022) 102940

Contents lists available at ScienceDirect

Journal of Autoimmunity

journal homepage: www.elsevier.com/locate/jautimm

Caspase-10 affects the pathogenesis of primary biliary cholangitis by regulating inflammatory cell death

Minjeong Cho [a,1], So Hee Dho [a,1], Saeam Shin [b,1], Yeongun Lee [a], Yoonjung Kim [b], Jiyeon Lee [a], Su Jong Yu [c], Sang Hoon Park [d,*], Kyung-A Lee [b,**], Lark Kyun Kim [a,***]

[a] Severance Biomedical Science Institute, Graduate School of Medical Science, Brain Korea 21 Project, Gangnam Severance Hospital, Yonsei University College of Medicine, Seoul, South Korea
[b] Department of Laboratory Medicine, Yonsei University College of Medicine, Seoul, South Korea
[c] Department of Internal Medicine and Liver Research Institute, Seoul National University College of Medicine, Seoul, South Korea
[d] Division of Gastroenterology and Hepatology, Department of Internal Medicine, Hallym University Kangnam Sacred Heart Hospital, Hallym University College of Medicine, Seoul, South Korea

ARTICLE INFO

Keywords:
Primary biliary cholangitis
Caspase-10
Autoimmunity
Inflammatory cell death
Exome sequencing

ABSTRACT

Primary biliary cholangitis (PBC) is an autoimmune disease that involves chronic inflammation and injury to biliary epithelial cells. To identify critical genetic factor(s) in PBC patients, we performed whole-exome sequencing of five female siblings, including one unaffected and four affected sisters, in a multi-PBC family, and identified 61 rare heterozygote variants that segregated only within the affected sisters. Among them, we were particularly interested in caspase-10, for although several caspases are involved in cell death, inflammation and autoimmunity, caspase-10 is little known from this perspective. We generated caspase-10 knockout macrophages, and then investigated the obtained phenotypes in comparison to those of its structurally similar protein, caspase-8. Unlike caspase-8, caspase-10 does not play a role during differentiation into macrophages, but after differentiation, it regulates the process of inflammatory cell deaths such as necroptosis and pyroptosis more strongly. Interestingly, caspase-10 displays better protease activity than caspase-8 in the process of RIPK1 cleavage, and an enhanced ability to form a complex with RIPK1 and FADD in human macrophages. Higher inflammatory cell death affected the fibrotic response of hepatic stellate cells; this effect could be recovered by treatment with UDCA and OCA, which are currently approved for PBC patients. Our findings strongly indicate that the defective roles of caspase-10 in macrophages contribute to the pathogenesis of PBC, thereby suggesting a new therapeutic strategy for PBC treatment.

1. Introduction

Primary biliary cholangitis (PBC) is a chronic liver disease characterized by destruction of small intrahepatic bile ducts, which subsequently progresses to fibrosis, cirrhosis, and liver failure [1]. PBC typically affects middle-aged females [2] and is regarded as a complex disorder caused by the interaction of immunological/environmental factors and genetic susceptibilities [3]. Autoantibodies to mitochondrial antigens and elevated immunoglobulin M levels are commonly found in the sera of patients with PBC, and hence, PBC is considered an autoimmune disease [1]. Especially, the anti-mitochondrial antibody targeting pyruvate dehydrogenase E2 complex is found in 90%–95% of PBC

Abbreviations: ALPS, autoimmune lymphoproliferative syndrome; CI, confidence interval; DED, death-effector domain; DEGs, differentially expressed genes; GSEA, gene set enrichment analysis; GWAS, genome-wide association studies; HSC, hepatic stellate cell; KO, knockout; OCA, obeticholic acid; OR, odd ratio; PCA, principal component analysis; PBC, Primary biliary cholangitis; UDCA, ursodeoxycholic acid; WES, whole-exome sequencing.

* Corresponding author.Division of Gastroenterology and Hepatology, Department of Internal Medicine, Hallym University Kangnam Sacred Heart Hospital, 1 Singil-ro, Yeongdeungpo-gu, Seoul 07441, South Korea.
** Corresponding author. Department of Laboratory Medicine, Yonsei University College of Medicine, 211 Eonju-ro, Gangnam-gu, Seoul 06273, South Korea.
*** Corresponding author. Severance Biomedical Science Institute, Graduate School of Medical Science, Brain Korea 21 Project, Gangnam Severance Hospital, Yonsei University College of Medicine, 20 Eonju-ro 63-gil, Gangnam-gu, Seoul 06230, South Korea.
E-mail addresses: sanghoon@hallym.or.kr (S.H. Park), KAL1119@yuhs.ac (K.-A. Lee), LKKIM@yuhs.ac (L.K. Kim).
[1] These authors contributed equally to this work.

https://doi.org/10.1016/j.jaut.2022.102940
Received 11 August 2022; Received in revised form 8 October 2022; Accepted 14 October 2022
Available online 27 October 2022

cases [1].

Presence of autoantibodies evokes the role of adaptive immunity in PBC, and indeed, the cellular adaptive immune system is involved in the onset, development, and prognosis of PBC [4]. However, since the immune system is precisely controlled by the interplay between innate and adaptive immunity, the role of the innate immune system should also be examined in the pathogenesis of PBC [4]. The fact that the damage in PBC is restricted to small biliary epithelial cells suggests the possibility that biliary epithelial cells translocate pyruvate dehydrogenase E2 complex to apoptotic bodies and then promote intense production of inflammatory cytokines from macrophages of patients with PBC [5]. Accumulating evidence shows that inflammation signaling in hepatic innate immunity contributes to liver injury, inflammation, and fibrosis [6]. Especially, hepatic macrophages promote liver fibrosis by enhancing survival of hepatic stellate cells (HSCs) [7]. In addition, the effect of accumulated environmental factors, including microorganisms, on the pathogenesis of PBC suggests the important role of the innate immune system [6].

Notably, the observation of familial occurrence, especially in female relatives, and of concordance in monozygotic twins suggests the contribution of genetic factors in the development of PBC [8]. However, studies investigating genetic factors that are possibly involved in PBC have not reported many leads: one study identified a weak association with a class II human leukocyte antigen, while another recent study showed the possible involvement of several risk loci-containing genes such as *TNFSF1A/8/15*, *STAT1/4*, *CXCR5*, *NF-kappaB1*, and *IL-12A/16/21* [9,10]. Moreover, it has been reported that *keratin 8/18/19* variants are associated with the severity of PBC in Italian patients [11] and that mitochondrial DNA variants increase the risk of late-onset PBC [12]. However, as observed in other autoimmune diseases, genome-wide association studies (GWAS) have identified that risk variants have subtle effects on PBC susceptibility [13], although the precise genetic mechanism of PBC is still unknown.

In the present study, we identified 61 rare heterozygote variants using whole-exome sequencing (WES) of samples from five female siblings, including an unaffected and four affected sisters, in a multi-PBC family. In the study focused on caspase-10, which is one of only two caspases that have two death-effector domain (DED) domains. The other DED-containing caspase is caspase-8, which has recently been studied extensively as a molecule that determines apoptosis and inflammatory cell deaths, such as necroptosis [14] and pyroptosis [15]. Unlike caspase-8, which exists both in mice and humans, caspase-10 exists only in humans, and has been thought to play a role similar to that of caspase-8; however, there are very few studies on caspase-10 [16].

In this study, we uncovered the role of caspase-10 in human macrophages, upon various stimuli. Unlike caspase-8, caspase-10 does not play a role during differentiation into macrophages; however, after differentiation, caspase-10 regulates the process of inflammatory cell deaths more strongly than caspase-8. The inflammatory cell deaths induced by the deletion or missense mutation of caspase-10 in macrophages were found to affect a fibrotic response of HSCs; this effect was recovered upon treatment with ursodeoxycholic acid (UDCA) and obeticholic acid (OCA), which are currently approved drugs for patients with PBC.

2. Material and methods

2.1. Study participants

We have previously published a report on the index PBC family (four affected sisters and an unaffected half-sister) [17]. The validation set is composed of 62 patients including 1) 23 patients with PBC diagnosed at Hallym University Kangnam Sacred Heart Hospital, Seoul, Korea and 2) 39 buffy coat samples from patients with PBC provided by the Seoul National University Hospital Human Biobank, Seoul, Korea. The study protocol was approved by the Ethics Committee of Hallym University Kangnam Sacred Heart Hospital (IRB No.2016-11-149), and informed consent was obtained from all participants. The diagnosis of PBC was made if at least two of the following three criteria were met: biochemical evidence of cholestasis, identified by elevated alkaline phosphatase levels; presence of serum anti-mitochondrial antibody; and histological evidence of non-suppurative destructive cholangitis and interlobular bile duct destruction [17].

2.2. Exome sequencing

Genomic DNA was extracted from buffy coat cells using the Easy-DNA™ gDNA Purification Kit (catalog no. K180001, Invitrogen, Carlsbad, CA, USA). WES was performed on the DNA samples of four affected sisters and one unaffected half-sister from a PBC family to identify the involved pathogenic mutations. The whole-exome was captured and enriched using the SureSelect Human All Exon V5 Kit (catalog no. Agilent Technologies, Santa Clara, CA, USA), following the manufacturer's standard protocol. The libraries were sequenced as 100 bp paired-end reads on a HiSeq 2500 sequencer (Illumina, San Diego, CA, USA). The raw sequence reads were mapped to the February 2009 human genome reference (GRCh37/Hg19) using the Burrows–Wheeler Aligner-Maximal Exact Match algorithm (version 0.7.12). PCR duplicates were removed with Picard. Indel realignment, base recalibration, and variant calling were carried out using the Genome Analysis Toolkit. Sequence variants, including single-nucleotide variants and insertion/deletions, were annotated using ANNOVAR.8. Among the coding variants that segregated only within the affected sisters, we filtered out (1) synonymous and (2) common variants (minor allele frequency>0.01) against public databases [1000 Genomes Project, genome Aggregation Database (gnomAD, http://gnomad.broadinstitute.org/), and Korean Reference Genome Database (http://coda.nih.go.kr/coda/KRGDB/index.jsp)]. The obtained candidate variants were again filtered by means of visual inspection of the mapped data using Integrated Genomics Viewer 2.3 software (Broad Institute). The remaining variants were further narrowed down using Online Mendelian Inheritance in Man (https://www.omim.org/).

2.3. Cell culture

U937 cells (catalog no. 21593.1, KCLB, Seoul, Korea) were maintained in RPMI-1640 medium (catalog no. 11875119, Gibco, Thermo Fisher Scientific, Waltham, MA, USA) supplemented with 10% fetal bovine serum (FBS; catalog no. 10099141, Gibco), 1% penicillin (catalog no. 15070063, Gibco), 1 × MEM-NEAA (catalog no. 11140050, Gibco), 1% L-glutamine (catalog no. 25030081, Gibco), 1% sodium pyruvate (catalog no. 11360070, Gibco), and 50 μM 2-mercaptoethanol (catalog no. M3148, Sigma-Aldrich, St. Louis, MO, USA). LX-2 (catalog no. SCC064, Merck, Darmstadt, Germany) and 293T (catalog no. CRL-3216, ATCC, Manassas, VA, USA) cells were grown in Dulbecco's modified Eagle medium (catalog no. SH30243.01, Hyclone, Rogan, UT, USA) supplemented with 10% FBS (catalog no. SH30084.03, Hyclone) and 1% penicillin. For quantification of pro-inflammatory cytokines, culture supernatants were collected and subjected to centrifugation, following which their levels were measured using enzyme-linked immunosorbent assay (ELISA) MAX™ Kits from BioLegend (San Diego, CA, USA) for human interleukin-1 beta (IL-1β; catalog no. 437004), tumor necrosis factor-alpha (TNF-α; catalog no. 430204), and IL-6 (catalog no. 430504).

2.4. Generation of caspase-10 and -8 knockout (KO) U937 cell lines using CRISPR/Cas9

CASP10 and *CASP8* guide RNAs (gRNAs) were designed using CHOPCHOP tool (http://chopchop.cbu.uib.no; Supplementary Table 1) [18]. The gRNAs were cloned into Lenti-CRISPRvr2 (catalog no. 52961, Addgene). To generate caspase-10 and -8 KO U937 cells,

Lenti-CRISPR-*CASP10* gRNA and Lenti-CRISPR-*CASP8* gRNA were electroporated into U937 using the Neon™ Transfection System (Life Technologies; 1400 V, 10 m s, and 3 pulses). After puromycin selection, the editing of *CASP10* and *CASP8* was confirmed using colony DNA PCR (Supplementary Table 2) and Sanger's sequencing.

2.5. RNA-sequencing (RNA-seq)

Total RNA samples were isolated using the RNeasy Mini Kit (catalog no. 74104, Qiagen, Hilden, Germany). The RNA seq data (GSE210070) was analyzed as described in the Supplementary Materials and Methods.

2.6. Caspase-10 activity

The catalytic activity of caspase-10 was measured using cleavage of its substrate, AEVD-pNA (catalog no. 1114, BioVision, Milpitas, CA, USA) or RIPK1. Serological measurement of caspase-10 activity was carried out using a microplate reader at a wavelength of 405 nm. Sera from 39 patients with PBC and 48 normal controls were diluted in the ratio of 1:1, in a buffer containing 10 mmol/L KCl, 50 mmol/L Tris-HCl (pH 7.4), and 5% glycerol. Following that, 100 μL of the diluted serum samples were incubated with 5 μL of the caspase-10 substrate AEVD-pNA, for 1 h at 37 °C and measured using a microplate reader. Cleavage of Flag-tagged RIPK1 in the cell lysates was assessed using immunoblotting with an anti-Flag antibody (catalog no. F3165, Sigma-Aldrich). Recombinant RIPK1 (catalog no. TP760433, Origene, Rockville, MD, USA) was subjected to reactions with 100 units of caspase-3, -8, and -10 (catalog nos. BML-SE169, BML-SE172, BML-SE174, respectively, Enzo Life Sciences, Farmingdale, NY, USA), for 24 h at 37 °C, in a kosmotrope-based buffer containing 20 mM PIPES (catalog no. P6757, Sigma-Aldrich), 100 mM NaCl (catalog no. S1072, Bioseasang, Korea), 10% sucrose (catalog no. 0335, Amresco, Boise, ID, USA), 10 mM DTT (catalog no. D9779, Sigma-Aldrich), 0.05% CHAPS (catalog no. 850500P, Sigma-Aldrich), and 1 M sodium citrate (catalog no. PHR1416, Sigma-Aldrich). Caspase was pre-incubated in 1 M sodium citrate buffer containing 1.6 M sodium citrate, 20 mM PIPES, and 100 mM NaCl for 30 min, at 37 °C. Cleaved RIPK1 was separated on a sodium dodecyl sulfate-polyacrylamide gel, followed by Coomassie Blue staining.

2.7. RIPK1 kinase assay

The recombinant RIPK1 (catalog no. VA7591, Promega, Madison, WI, USA) was incubated with caspase-3, -8, or -10 (catalog nos. BML-SE169, BML-SE172, BML-SE174, respectively, Enzo Life Sciences) for 24 h at 37 °C in the caspase reaction buffer. The luminescence was measured to calculate the kinase activity after the addition of ADP-Glo Kinase assay following the manufacturer's instructions (catalog no. V9101, Promega).

2.8. Gel-filtration chromatography

293T cells were transiently transfected with pcDNA3.1-Myc-Casp10^{C401A}, pcDNA3.1-Myc-Casp8^{C360S}, pcDNA3.1-Flag-RIPK1, or pcDNA3.1-HA-FADD, for 24 h. Cells were lysed on ice in radioimmunoprecipitation assay lysis buffer containing protease inhibitor. Cell lysates were centrifuged at 13,000 rpm for 10 min, followed by collection of the supernatant. Gel-filtration was performed using AKTA™ FPLC (GE Healthcare, Chicago, IL, USA) and HiLoad® 16/600 Superdex® 200 Prep-grade Column (catalog no. 17-1043-02, GE Healthcare).

2.9. Statistical analysis

Statistical analysis was performed using SPSS version 24.0.0 (IBM). To assess the association between the *CASP10* genotype and PBC risk in patients *versus* controls, odds ratio (OR) and 95% confidence interval (CI) were calculated using chi-square test. Genotype frequency data of the controls were adapted from the East-Asian frequencies in gnomAD. Statistical analysis for all other experiments, unless otherwise indicated, was carried out using Student's *t*-test. $P < 0.05$ was considered statistically significant (*$P < 0.05$, **$P < 0.01$, and ***$P < 0.001$, *vs.* control).

3. Results

3.1. WES identified missense CASP10 variants in patients with PBC

To identify plausible genetic factor(s) involved in PBC, we performed WES on samples from five female siblings, including one unaffected and four affected sisters, in a multi-PBC family, at a mean depth of 157.3–233.7 × (99.3%–99.5% coverage, >10-fold) (Fig. 1A). After exclusion of synonymous variants, common variants, and sequencing artifacts, 61 rare heterozygote variants (missense, nonsense, indel, and splice site variants) that segregated only within the affected sisters were identified (Table 1). We hypothesized that these rare variants had a functionally significant impact on the development of PBC.

Among these variants, we particularly focused on caspase-10, because while caspases such as caspase-1, caspase-4, caspase-5, caspase-8 and caspase-11 are involved in cell death, inflammation and autoimmunity [19,20], the role of caspase-10 is little known in this context. The fact that the missense mutation [c.332G > C, p. Arg111Thr (R111T); dbSNP ID: rs199600895] in *CASP10* (MIM 601762; RefSeq accession number: NM_032977.3) is located in a linker segment between two DEDs was also interesting to us, considering that DED is a protein-interacting domain of many caspases and FADD, and regulates various cellular signaling cascades (Table 1 and Fig. 1B). To further confirm the role of caspase-10 in PBC, we performed Sanger's sequencing for *CASP10* using 62 additional unrelated patients with PBC, which resulted in the identification of three other rare variants in three sporadic patients (Supplementary Figure 1A). Interestingly, a newly discovered missense variant [c.314T > C, p. Leu105Pro (L105P); dbSNP ID: rs200530667] was also located in the same linker segment as the variant R111T found in the index family. A splice site variant (c.578-3C > T; dbSNP ID: rs759671327) and a synonymous variant (c.1519C > T, p. Leu507Leu; dbSNP ID: rs763149790) were identified in two patients. On the above basis, the frequency of the *CASP10* rare variant was calculated to be 4.84% (3/62 patients, excluding affected sisters of an index patient) in our PBC cohort. The odds ratio for the *CASP10* rare variant in patients with PBC (including an index patient in a PBC family) *versus* controls was 9.888 (95% CI, 3.130–31.235 and $P = 0.002$).

Upon pathogenicity prediction of the missense variants using sorting intolerant from tolerant (SIFT) and Polymorphism Phenotyping version 2 (PolyPhen-2), SIFT predicted caspase-10^{R111T} to be probably deleterious, while PolyPhen-2 predicted that caspase-10^{L105P} has a tolerable effect on the gene product (Table 1 and Supplementary Table 3). Additionally, the splice site variant (c0.578-3C > T) was predicted to potentially affect splicing, because it resulted in the creation of an exonic splicing silencer or alteration of an exonic splicing enhancer. The synonymous variant (c.1519C > T, p. Leu507Leu) showed a high genomic evolutionary rate profiling rejected substitution (RS) score (RS > 4), suggesting that it could be a putative functional variant (Supplementary Figure 1A). Furthermore, we performed computational structure prediction of *CASP10* variants using I-TASSER server (https://zhanglab.ccmb.med.umich.edu/I-TASSER/) and Alphafold2 (https://colab.research.google.com/github/deepmind/alphafold/blob/main/notebooks/AlphaFold.ipynb). These predicted that both the variants changed the secondary structure around the linker segment between the two DEDs (Supplementary Fig. 1B and C).

There are no previous studies on the potential role of caspase-10 in PBC pathogenesis. Therefore, we assessed whether the role of caspase-10 is applicable on a wide range of patients with PBC, and not restricted only to our multi-PBC family case. To test this, we measured caspase-10

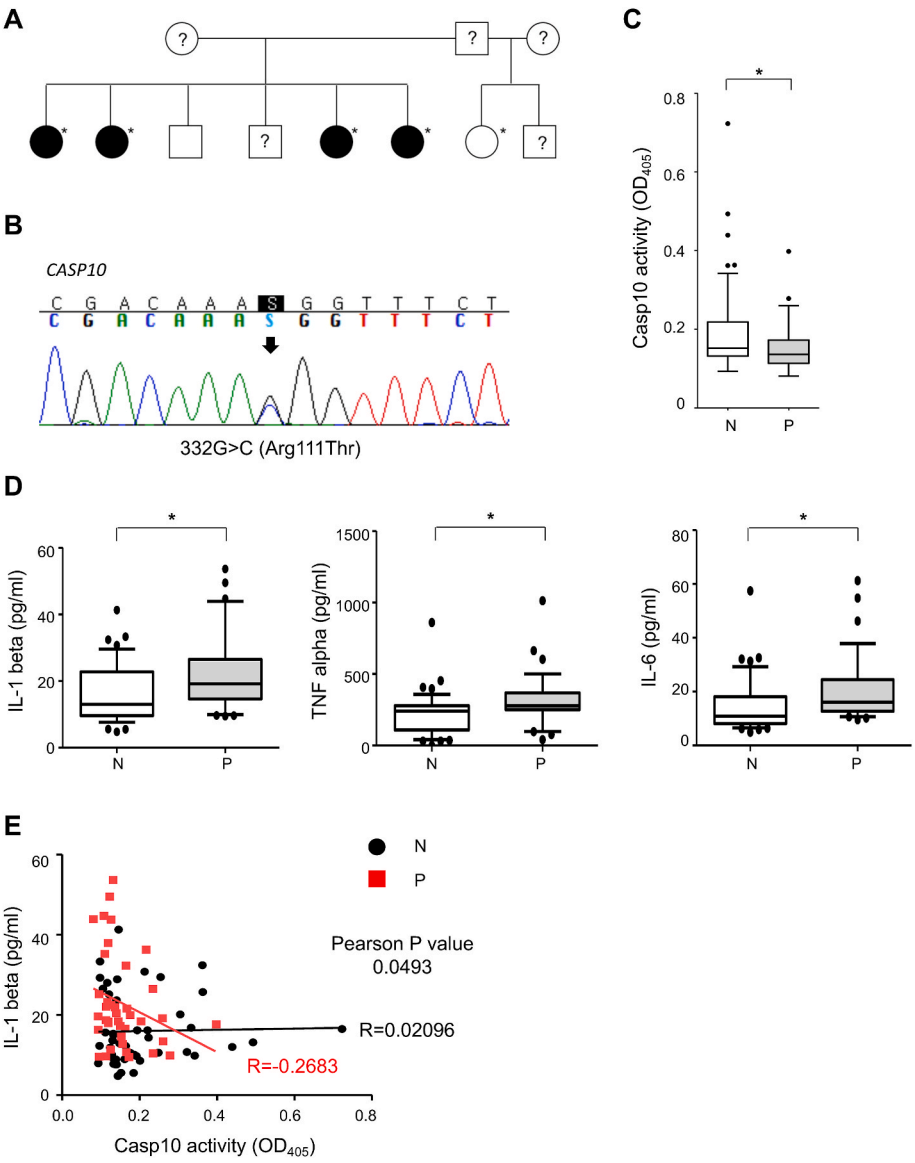

Fig. 1. A missense *CASP10* variant was identified by means of WES, in a multi-PBC family. (A) Pedigree of the multi-PBC family with four clinically affected sisters. The black circles indicate PBC-affected sisters, while the white symbols indicate non-affected family members. An asterisk indicates that WES was performed. A question mark indicates an individual with no phenotypic information. (B) Sanger's sequencing identified a rare variant in *CASP10* (NM_032977.3: c.332G > C, NP_116759.2:p.Arg111Thr) (arrow) in the multi-PBC family. (C) Caspase-10 activity in the sera from normal (N) or patients with PBC (P) (*P < 0.05 *vs.* normal, Student's *t*-test). Boxes indicate the 75th percentile, median, and 25th percentile. (D) Pro-inflammatory cytokines, including IL-1β, TNF-α, and IL-6 in sera of patients with PBC. Pro-inflammatory cytokines were assessed using ELISA. (E) Negative correlation between caspase-10 activity and levels of IL-1β in serum samples of patients with PBC.

activity in the sera from 39 patients with PBC and 48 age-matched normal controls, and found that the patients with PBC showed decreased caspase-10 activity (Fig. 1C and Supplementary Table 4). Therefore, we concluded that reduced caspase-10 activity could be a feature of patients with PBC.

We next assessed the amounts of pro-inflammatory cytokines in the serum samples of patients with PBC, and found that IL-1β, TNF-α, and IL-6 are induced in the sera of patients with PBC (Fig. 1D). This result is in agreement with other reports demonstrating that PBC is characterized by elevated levels of pro-inflammatory cytokines when compared to controls [21]. Notably, there is an inverse correlation between caspase-10 activity and the levels of IL-1β, indicating that the decreased caspase-10 activity in patients with PBC could be attributed to up-regulation of pro-inflammatory cytokines (Fig. 1E). This inverse correlation is not specific for TNF-α or IL-6, but for IL-1β (Fig. 1E and Supplementary Fig. 2A and B).

3.2. *The proliferation rates of caspase-10 KO cells are similar to those of control cells, during differentiation to macrophages*

We generated KO cells to carry out functional validation of the roles of caspase-10. Considering that inflammation signaling in hepatic innate immunity contributes to liver injury, inflammation, and fibrosis, and that many caspases are well known for their roles in cell death and inflammation in myeloid cells, we decided to use human U937 monocytes for this study. The 5′ region of the *CASP10* exon 2 (Supplementary Figure 3A) was deleted in U937 cells using CRISPR/Cas9 editing. In the present study, we carried out a comparative analysis between caspase-8 and caspase-10, for the following reasons: i) these are the only two caspases that have two DED domains; ii) caspase-10 exists only in human cells; and iii) many studies have elucidated the functions of caspase-8 using KO mouse model systems, and owing to its structural similarity to caspase-8, caspase-10 is believed to have a similar role (Supplementary Figure 3B). Thus, we generated both caspase-10 and caspase-8 KO cells in the present study (Fig. 2A).

Further, we differentiated U937 monocytes into macrophages using phorbol 12-myristate 13-acetate (PMA), before subjecting them to immune stimuli [22]. Interestingly, before differentiation or any immunological stimulation, upon analysis using a live-cell proliferation assay, caspase-10 KO cells showed no significant difference from control cells, whereas caspase-8 KO cells showed a dramatic reduction (Fig. 2B–C). When we treated the cells with PMA for differentiation into macrophages, we found that caspase-10 KO cells still showed no significant difference from control cells in terms of cell viability, as assessed using

Table 1
List of variants that were identified by WES in a multi-PBC family.

Gene	GRCh37 chr:location	Transcript	cDNA change	Protein change	1000G_EAS_MAF	gnomAD_EAS_MAF	KRGDB_MAF	SIFT
CASP10	chr2:202050832	NM_032977.3	c.332G > C	p.Arg111Thr	0.001	0.0001091	N.A.	Deleterious
FUT2	chr19:49206674	NM_000511.5	c.461G > A	p.Trp154*	0.004	0.0022130	0.0008	N.A.
FUT2	chr19:49206985	NM_000511.5	c.772G > A	p.Gly258Ser	0.004	0.002160	0.0008	Tolerated
BMX	chrX:15560220	NM_001721.6	c.1510C > G	p.His504Asp	N.A.	N.A.	N.A.	Deleterious
FCRL4	chr1:157551369	NM_031282.2	c.1201C > T	p.Leu401Phe	0.003	0.002460	0.004	Tolerated
LILRA1	chr19:55107747	NM_006863.3	c.1052C > T	p.Pro351Leu	0.000	0.0001002	N.A.	Tolerated
LYVE1	chr11:10580792	NM_006691.3	c.835G > A	p.Glu279Lys	0.000	0.000	N.A.	Deleterious
SERPINA7	chrX:105280961	NM_000354.5	c.89G > T	p.Cys30Phe	N.A.	0.000	N.A.	Tolerated
SIGLEC8	chr19:51960733	NM_014442.2	c.715G > A	p.Val239Ile	N.A.	0.0008019	0.0024	Tolerated
TPTE2	chr13:20066994	NM_199254.2	c.115A > G	p.Lys39Glu	N.A.	N.A.	0.0008	Tolerated
TRIM32	chr9:119460430	NM_001099679.1	c.409C > T	p.Pro137Ser	0.003	0.004110	0.0024	Tolerated
USP2	chr11:119243857	NM_004205.4	c.334G > A	p.Gly112Arg	0.002	0.0008156	0.0024	Tolerated
EXOC3L4	chr14:103568706	NM_001077594.1	c.646C > A	p.Arg216Ser	0.0079	0.000000	0.0072	Tolerated
MET	chr7:116339827	NM_001127500.1	c.689C > T	p.Thr230Met	N.A.	0.000	0.0008	Tolerated
ARMC6	chr19:19153665	NM_001199196.1	c.175G > A	p.Val59Met	0.003	0.001153	0.0016	Tolerated
DKK2	chr4:107845768	NM_014421.2	c.463T > C	p.Tyr155His	N.A.	0.001855	0.0064	Tolerated
PRIM2	chr6:57512788	NM_000947.4	c.*85 + 1_*85+2insTA	.	N.A.	N.A.	N.A.	N.A.
PRB2	chr12:11546866	NM_006248.3	c.146G > A	p.Gly49Asp	0.000	0.000251	N.A.	Tolerated
USP37	chr2:219346901	NM_020935.2	c.1727A > G	p.Asn576Ser	N.A.	0.0004350	0.0024	Tolerated
URM1	chr9:131140355	NM_001135947.2	c.76C > T	p.Arg26*	N.A.	0.000	N.A.	N.A.
WHAMM	chr15:83478751	NM_001080435.2	c.273C > A	p.His91Gln	N.A.	N.A.	N.A.	Deleterious
ZSCAN5B	chr19:56701449	NM_001080456.2	c.1235T > C	p.Met412Thr	0.001	0.001206	0.0032	Tolerated
ZNF292	chr6:87969411	NM_015021.1	c.6064G > C	p.Ala2022Pro	N.A.	0.001119	0.008	Tolerated
ZNF614	chr19:52519848	NM_025040.3	c.1003C > T	p.Arg335*	N.A.	0.0001002	0.0008	N.A.
ZNF683	chr1:26694282	NM_001114759.1	c.121T > G	p.Ser41Ala	N.A.	0.000059	N.A.	Tolerated
ZNF865	chr19:56127308	NM_001195605.1	c.2324G > A	p.Gly775Glu	N.A.	0.000197	0.0008	Tolerated
CSNK2A3	chr11:11373951	NM_001256686.1	c.716A > G	p.Tyr239Cys	N.A.	0.000301	N.A.	Tolerated
ERVV-2	chr19:53553255	NM_001191055.1	c.751C > G	p.Pro251Ala	N.A.	N.A.	0.0008	Damaging
FAM110D	chr1:26488419	NM_024869.2	c.637T > C	p.Ser213Pro	N.A.	0.001421	0.000909	Tolerated
FER1L6	chr8:125109581	NM_001039112.2	c.4765T > G	p.Ser1589Ala	N.A.	N.A.	N.A.	Deleterious
GRTP1	chr13:114009787	NM_001286732.1	c.191A > G	p.Tyr64Cys	N.A.	0.000050	N.A.	Deleterious
HECW2	chr2:197183524	NM_020760.1	c.2090C > T	p.Ser697Leu	0.000	0.000	N.A.	Tolerated
KCNJ14	chr19:48968015	NM_013348.3	c.1292C > T	p.Ala431Val	0.000	0.000352	0.000455	Tolerated
LMNTD1	chr12:25672898	NM_001145728.2	c.910T > A	p.Phe304Ile	N.A.	0.000272	0.0016	Deleterious
MROH7	chr1:55175825	NM_001039464.3	c.3937G > C	p.Ala1313Pro	0.0069	0.001782	0.0056	Deleterious
OR52B2	chr11:6190850	NM_001004052.1	c.707G > A	p.Arg236Gln	0.0099	0.008406	0.0088	Tolerated
OR52W1	chr11:6221249	NM_001005178.1	c.796A > G	p.Thr266Ala	0.0099	0.008821	0.0088	Tolerated
OR8G5	chr11:124135428	NM_001005198.1	c.706A > G	p.Ile236Val	N.A.	0.000110	0.0008	Tolerated
PRKRIP1	chr7:102065554	NM_024653.3	c.551G > A	p.Arg184Gln	0.003	0.000383	0.0008	Deleterious
SRSF12	chr6:89808481	NM_080743.4	c.602A > G	p.Gln201Arg	0.000	0.002355	0.0024	Tolerated
TTC27	chr2:32897361	NM_017735.4	c.962C > G	p.Thr321Ser	N.A.	0.000	N.A.	Deleterious
TTLL4	chr2:219617567	NM_014640.4	c.3058C > T	p.Arg1020Cys	N.A.	N.A.	N.A.	Tolerated
CTNNA2	chr2:80085156	NM_001282597.1	c.316G > A	p.Ala106Thr	0.001	0.001126	0.0008	Tolerated
CLCNKA	chr1:16359717	NM_004070.3	c.1982G > C	p.Arg661Pro	N.A.	0.000752	0.0024	Tolerated
CCDC114	chr19:48800751	NM_144577.3	c.1495G > T	p.Ala499Ser	0.003	0.000210	0.000455	Tolerated
CSF3R	chr1:36941110	NM_156039.3	c.229C > T	p.Arg77Cys	N.A.	N.A.	N.A.	Tolerated
DCHS1	chr11:6651101	NM_003737.3	c.4837G > A	p.Ala1613Thr	N.A.	0.000276	0.0016	Tolerated
EPG5	chr18:43526693	NM_020964.2	c.1613G > A	p.Arg538Gln	0.000	0.0008701	0.0032	Tolerated
EPS8L1	chr19:55597526	NM_133180.2	c.1616G > A	p.Arg539Gln	0.002	0.000908	0.004	Tolerated
EPS8L1	chr19:55598675	NM_133180.2	c.1957G > T	p.Val653Leu	N.A.	0.000809	0.004	Deleterious
IKBKAP	chr9:111679946	NM_003640.3	c.745T > C	p.Ser249Pro	N.A.	0.000652	0.0016	Deleterious
MRVI1	chr11:10622597	NM_130385.3	c.1885A > G	p.Met629Val	N.A.	0.000	N.A.	Tolerated
NCOR1	chr17:15968277	NM_006311.3	c.5008A > G	p.Thr1670Ala	0.004	0.003007	0.0096	Tolerated
OBSL1	chr2:220430093	NM_015311.2	c.2278G > A	p.Glu760Lys	N.A.	0.000512	0.0008	Deleterious
PAPPA	chr9:119144750	NM_002581.3	c.4754C > T	p.Thr1585Ile	0.005	0.007322	0.0064	Deleterious
PRSS56	chr2:233390022	NM_001195129.1	c.1618G > A	p.Val540Met	N.A.	N.A.	N.A.	Damaging
RELN	chr7:103193944	NM_005045.3	c.6036C > G	p.Asp2012Glu	0.001	0.0001088	0.0008	Tolerated
SFMBT2	chr10:7213936	NM_001018039.1	c.2336G > A	p.Arg779Gln	0.002	0.000739	0.0024	Deleterious
SEZ6L	chr22:26688507	NM_021115.4	c.230C > T	p.Ala77Val	0.003	0.003764	0.0032	Deleterious
SCNN1D	chr1:1226063	NM_001130413.3	c.1906G > A	p.Ala636Thr	0.0099	0.007177	0.0032	Tolerated
TEAD1	chr11:12904623	NM_021961.5	c.650G > A	p.Arg217His	0.002	0.002656	0.0072	Deleterious

Chr, chromosome; 1000G_EAS_MAF, East-Asian minor allele frequency in 1000 Genomes Project; gnomAD_EAS_MAF, East-Asian minor allele frequency in genomAD exome database; KRGDB_MAF, Korean minor allele frequency in the Korean Reference Genome Database; N.A.; not available.

PI staining and Trypan Blue exclusion assay, while caspase-8 KO cells still showed a significant reduction in cell viability (Fig. 2D–F). Thus, we concluded that caspase-8 regulates cell proliferation or viability, even at steady state, but caspase-10 does not.

3.3. Inflammatory cytokine genes are more induced in caspase-10 KO macrophages, upon immune stimulation

To explore the role of caspase-10, we performed RNA-seq using samples from caspase-10 or caspase-8 KO U937 macrophages, upon immune stimulation such as that with lipopolysaccharide (LPS), TNF-α, or Z-VAD + cycloheximide + TNF-α (ZCT). We executed RNA-seq with triplicates of each sample and performed PCA (Supplementary

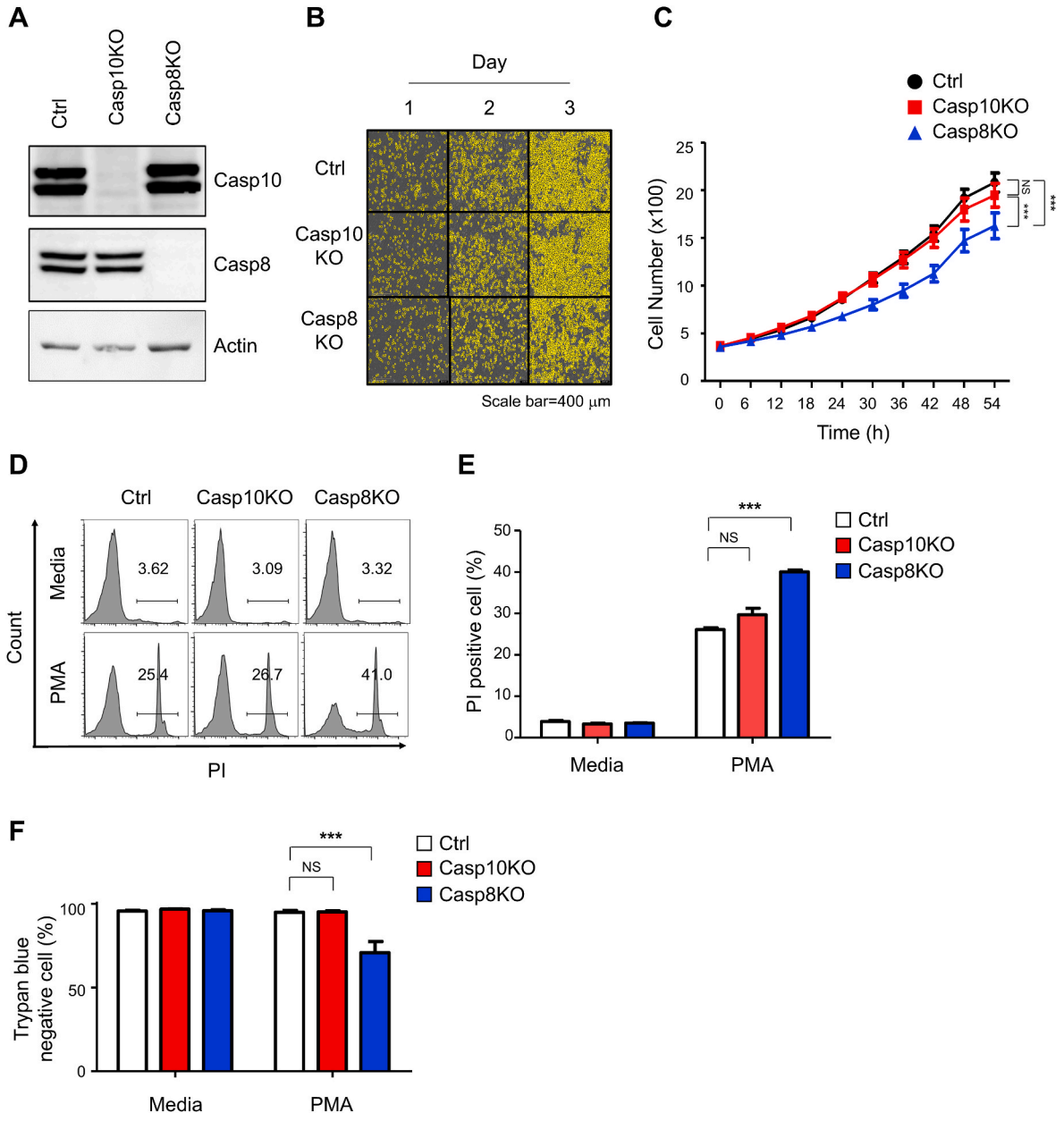

Fig. 2. Cell proliferation in the caspase-10 knockout (Casp10 KO) cells differs significantly from that in caspase-8 knockout (Casp8 KO) cells. (A) Assessment of Casp10 and Casp8 deletion using immunoblotting, in control (Ctrl), Casp10 KO, and Casp8 KO U937 cells. (B–C) IncuCyte® cell proliferation assay of Ctrl, Casp10 KO, and Casp8 KO U937 cells. Results are presented as mean ± SEM (error bars) (n = 3; ***P < 0.001 *vs.* Ctrl or Casp8 KO, Student's *t*-test). (D–E) PI-stained cell death assay of media- or PMA-treated Ctrl, Casp10 KO, and Casp8 KO macrophages (n = 3). (F) Trypan Blue exclusion assay of media- or PMA-treated Ctrl, Casp10 KO, and Casp8 KO U937 cells (n = 3).

Fig. 4A–C). We found that the presence or absence of differentiation or immune stimulation leads to far greater transcriptomic alterations than genetic differences of caspase-8 or caspase-10. Next, we analyzed the transcriptomic changes before and after PMA treatment-induced differentiation into macrophages, and also looked at the changes after LPS stimulation, using caspase-10 or caspase-8 KO cells. DEGs (>2-fold expression differences and <0.05 *P*-value) were classified into 7 clusters using K-means clustering (Fig. 3A). Among them, we noted that cluster III genes were induced by PMA only in caspase-8 KO macrophages. The genes in Cluster III included pro-apoptotic factors such as kruppel-like factor 4 (*KLF4*) [23] and *CHAC1* [24] (Fig. 3B). GSEA showed that Cluster III was enriched in genes related to regulation of immune system process and cell death, including apoptosis (Fig. 3C), thereby providing a possible reason for why the PMA-treated caspase-8 KO cells were susceptible to cell death, but the caspase-10 KO cells were not (Fig. 2D–F).

We next observed that the Cluster V genes were induced by PMA and LPS in caspase-10 KO cells. Cluster V consisted of critical inflammatory genes, including *IL-1β*, *IL-6*, and *TNF-α* (Fig. 3B). Gene Ontology analysis revealed enriched terms such as response to cytokine, myeloid leukocyte activation, and regulation of cell death, especially in LPS-treated caspase-10 KO macrophages in Cluster V (Fig. 3D). These findings were consistent with the results of GSEA, which indicated augmented expression of genes involved in inflammatory response ($P < 0.0001$) and positive regulation of lymphocyte-mediated immunity ($P < 0.0001$) (Fig. 3E). To confirm whether the RNA-seq results reflect the pattern of RNA expression, we checked the expression of the representative genes using real-time quantitative PCR (Supplementary Fig. 5A and B).

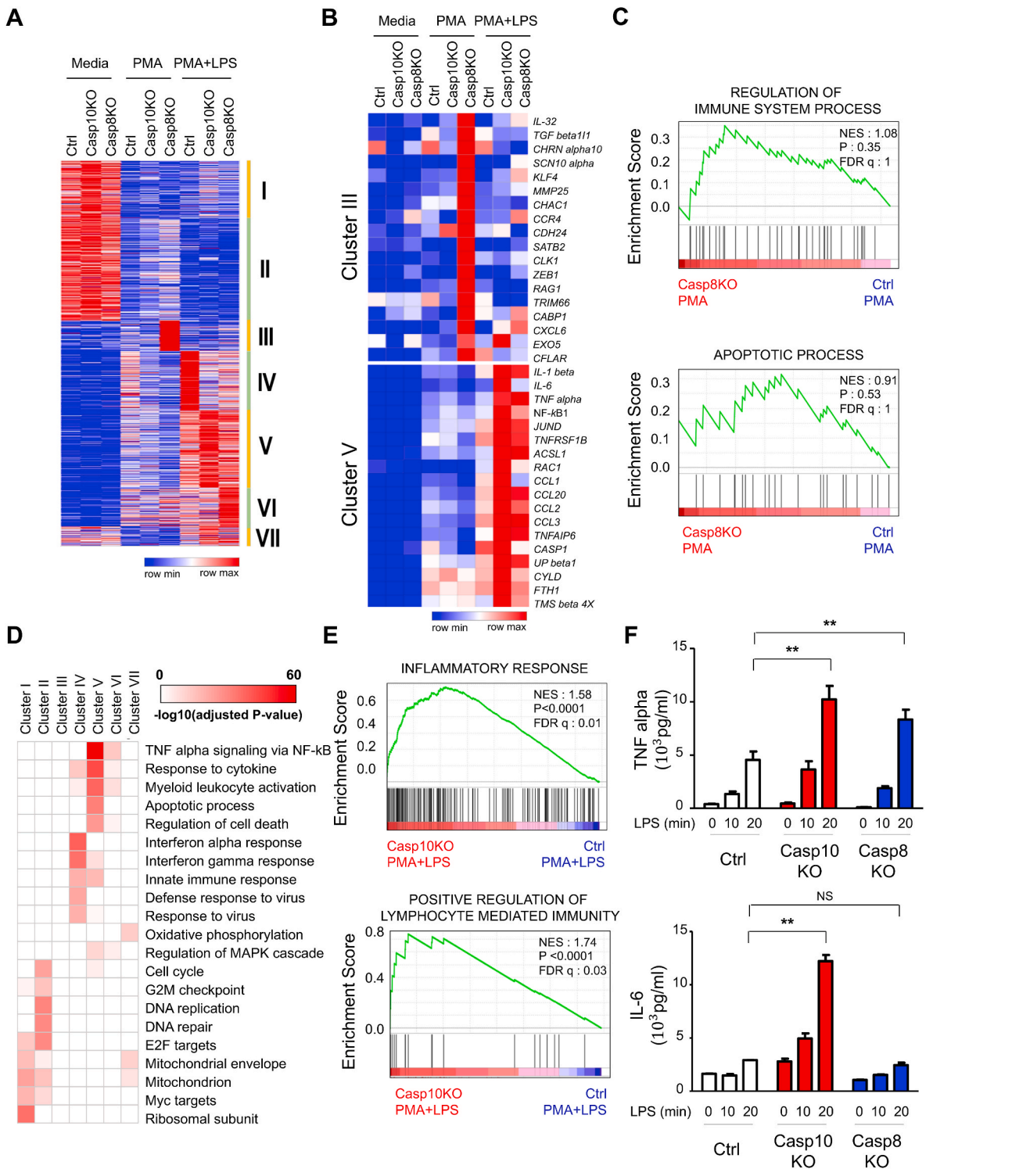

Fig. 3. RNA-seq analysis revealed upregulation of inflammatory signaling molecules in caspase-10 knockout (Casp10 KO) macrophages. (A) RNA-seq data analysis using K-means clustering of control (Ctrl), Casp10 KO, and caspase-8 knockout (Casp8 KO) U937 cells in media-, PMA (10 nM of PMA overnight)-, or PMA + LPS (PMA followed by 1 μg/mL of LPS for 3 h)-treated conditions. (B) Representative genes of Clusters III and V are indicated on the right. (C) Heat-maps of significant Gene Ontology terms in each cluster. GSEA enrichment plots of (D) Cluster III and (E) Cluster V. (F) ELISA for TNF-α (n = 4) and IL-6 (n = 3) release from untreated or LPS-treated Ctrl, Casp10 KO, and Casp8 KO macrophages (**P < 0.01 *vs.* Ctrl, as assessed using Student's *t*-test).

Furthermore, we assessed TNF-α and IL-6 production using ELISA (Fig. 3F). These assays indicated that caspase-10 KO macrophages show enhanced expression levels of pro-inflammatory cytokines such as TNF-α, IL-1β, and IL-6, upon LPS stimulation.

Additionally, when we checked the transcriptomic changes after TNF-α stimulation, using caspase-10 or caspase-8 KO cells, we obtained similar results for gene cluster pattern, as those obtained upon LPS stimulation (Supplementary Figure 6A). Of the nine clusters that were obtained upon K-means clustering, we focused on Cluster VII genes, which were induced by PMA and TNF-α in caspase-10 KO macrophages. These genes consisted of inflammatory genes, including *TNF-α*, *IL-6*, and *IL-1β* (Supplementary Figure 6B). Gene Ontology analysis revealed

strong signals for terms such as response to cytokine, myeloid leukocyte activation, and TNF-α signaling *via* NF-kB, especially in TNF-α-treated caspase-10 KO macrophages (Supplementary Figure 6C). GSEA revealed that there is upregulation in the genes associated with positive regulation of immune effector processes and inflammatory response in caspase-10 KO cells treated with TNF-α (Supplementary Figure 6D).

3.4. There is greater IL-1β production, inflammasome formation, and inflammatory cell death in caspase-10 KO macrophages, upon LPS and s.ig stimulation

The finding that the level of IL-1β has significant negative correlation with caspase-10 activity in sera of patients with PBC led us to check caspase-1 activation, formation of inflammasome complex, and GSDMD cleavage [25] in caspase-10 KO macrophages, upon LPS and Nig stimulation. Immunoblotting and ELISA revealed that caspase-10 KO macrophages showed more caspase-1 activation and IL-1β production than control cells, after LPS and Nig stimulation (Fig. 4A–B). Caspase-8 KO cells also showed a similar pattern of more caspase-1 activation and IL-1β production, as compared to control cells, although the degree of elevation was little lower than that observed in caspase-10 KO cells (Fig. 4A–B). Moreover, we checked ASC oligomerization and observed more formation of ASC proteins in caspase-10 and caspase-8 KO cells (Fig. 4C). There was also an increase in the cleavage of GSDMD (which is carried out by the inflammasome complex) in caspase-10 and caspase-8 KO cells (Fig. 4D).

Because it is well known that cleaved GSDMD causes pyroptosis by forming membrane pores [25], which leads to inflammatory cell death that triggers immune reactions of adjacent cells, we wanted to further confirm that there is enhanced cell death in caspase-10 KO macrophages only after LPS and Nig stimulation. We then found enhanced LDH release and cell deaths, as measured by means of live-cell death assay and PI/Annexin V staining, in caspase-10 and caspase-8 KO macrophages (Fig. 4E–H). Again, caspase-8 KO cells showed a similar pattern of cell death extent as caspase-10 KO cells, upon LPS and Nig stimulation, but unlike caspase-10 KO cells, the death of caspase-8 KO cells already began before stimulation (Fig. 4G–H), which is consistent with the observation that caspase-8 cells underwent more death during differentiation into macrophages (Figs. 2 and 3).

3.5. There is more necroptosis in caspase-10 KO macrophages after ZCT treatment

We investigated the role of caspase-10 in another inflammatory cell death, *i.e.*, necroptosis. Since caspase-8 is well known to inhibit necroptosis mediated by RIPK1, RIPK3, and MLKL [26], we wanted to compare caspase-10 KO macrophages to caspase-8 cells after ZCT treatment. RNA-seq analysis resulted in eight clusters, as classified by means of K-means clustering (Fig. 5A), and among them, we particularly focused on Cluster VI and VII genes, which were induced in caspase-10 and caspase-8 KO cells after ZCT treatment, respectively. Cluster VI consisted of inflammatory genes including *TNF-α*, *IL-1β*, and *IL-6*, while Cluster VII consisted of *CXCL1*, *CXCL2*, and *CCL8* (Fig. 5B). Additionally, Gene Ontology analysis showed the enrichment of signal cascades such as response to cytokines, myeloid leukocyte activation, and regulation of cell death in Cluster VI; these were also enriched in Cluster VII, albeit to a lesser degree (Fig. 5C).

We next investigated the activation of RIPK1, RIPK3, and MLKL, by measuring the phosphorylation level of each protein in caspase-10 and caspase-8 KO cells after ZCT treatment. We found that there were higher levels of phosphorylated RIPK1, RIK3, and MLKL in caspase-10 KO macrophages as well as caspase-8 KO macrophages, after ZCT treatment (Fig. 5D). We also confirmed by means of live-cell death assay and PI/Annexin V staining that there was enhanced LDH release and cell death in the caspase-10 and caspase-8 KO macrophages (Fig. 5E–H). Caspase-8 KO cells showed a similar pattern of cell death extent as caspase-10 KO cells after ZCT treatment, but unlike caspase-10 KO cells, the death of caspase-8 KO cells already began before stimulation (Fig. 5E–H).

3.6. Caspase-10 displays greater enzymatic activity for cleavage of RIPK1 than caspase-8

In the system consisting of human macrophage cells differentiated from U937 monocytes, caspase-8 showed a clear difference, as compared to caspase-10, in terms of cell viability during differentiation into macrophages. But post differentiation and adjustment of cell numbers for further stimulation in a relatively limited period, caspase-8 and caspase-10 showed very similar patterns, of higher expression levels of inflammatory cytokines and extents of inflammatory cell deaths, as measured in terms of GSDMD cleavage, MLKL phosphorylation, *etc*.

The two caspases were directly compared in terms of their binding ability to target proteins and enzymatic activity to cleave target proteins. It is well known that caspase-8 binds to FADD and RIPK1, resulting in the formation of the necroptosis complex upon TNF-α stimulation [27]. Thus, we checked whether caspase-8 makes a complex with FADD and RIPK1 in caspase-10 KO macrophages. Interestingly, we found that there are more bindings among these three proteins in caspase-10 KO macrophages after ZCT treatment, even though there was no observation of such bindings in control cells (Fig. 6A). To reveal the direct correlation between caspase-10 or caspase-8 and RIPK1, we transfected HEK 293 cells to express these proteins. When we transfected the cells with wild-type caspase-10 or caspase-8, we failed to observe RIPK1 expression, which is seen upon the enzymatic cleavage of RIPK1 by the two proteins (Fig. 6B). Thus, we generated enzymatic dead caspase-10 and caspase-8, that are caspase-10^{C401A} and caspase-8^{C360S}, respectively [28,29], and transfected the cells with these mutant constructs. Upon doing so, we detected RIPK1 expression, thereby suggesting that both caspase-10 and caspase-8 cleave RIPK1 (Fig. 6B). To check the direct interaction between caspase-10 or caspase-8 and RIPK1, we again transfected the cells with RIPK1, FADD, and mutant caspase-10 or mutant caspase-8, and then performed co-immunoprecipitation with RIPK1 (Flag-tagged). We found that RIPK1 and FADD directly interact with caspase-10 or caspase-8 in a dose-dependent manner (Fig. 6C), and moreover, confirmed that caspase-10 and caspase-8 can make a complex with RIPK1 and FADD using gel-filtration chromatography (Fig. 6D). Next, we checked whether there was a difference between caspase-10 and caspase-8 in terms of their binding preferences with RIPK1. When we transfected RIPK1, FADD, caspase-10, and caspase-8 simultaneously, with either caspase-10 or caspase-8 in a fixed dose and the other in a dose-dependent manner, we found that RIPK1 binds with caspase-10 or caspase-8, without any preference for either protein (Supplementary Fig. 7A–C).

Further, we investigated whether there was a difference between the two proteins in terms of their ability to cleave RIPK1. For this, we purchased recombinant caspase-10, caspase-8, and caspase-3 proteins from Enzo Life Sciences, and assayed whether RIPK1 is cleaved by the recombinant caspases *in vitro*. We used a kosmotrope-based assay [30] to determine that caspase-10 contributes more to the RIPK1 proteolytic process than caspase-8 (Fig. 6E–F). To further confirm the superior cleavage ability of caspase-10, we generated a mutant RIPK1 (RIPK1^{D324A}), which is not cleaved by caspase-10 and caspase-8, and then incubated the wild-type or mutant form of RIPK1 with the recombinant caspase-10, caspase-8, or caspase-3 *in vitro*. The results confirmed that caspase-10 cleaves RIPK1 more efficiently than caspase-8 (Supplementary Figure 7D). Furthermore, since the possible cleavage sites in RIPK1 at which caspase-10 acts include D180 and D324 [31], and the D180 site is located in the kinase domain, we considered the possibility that the kinase activity of RIPK1 is reduced upon caspase-10 cleavage. We performed ADP-Glo kinase assay and found that there was a significant decline in the RIPK1 kinase activity upon caspase-10 treatment (Supplementary Figure 7E). Thus, we concluded that caspase-10 displayed greater enzymatic activity to cleave RIPK1 than

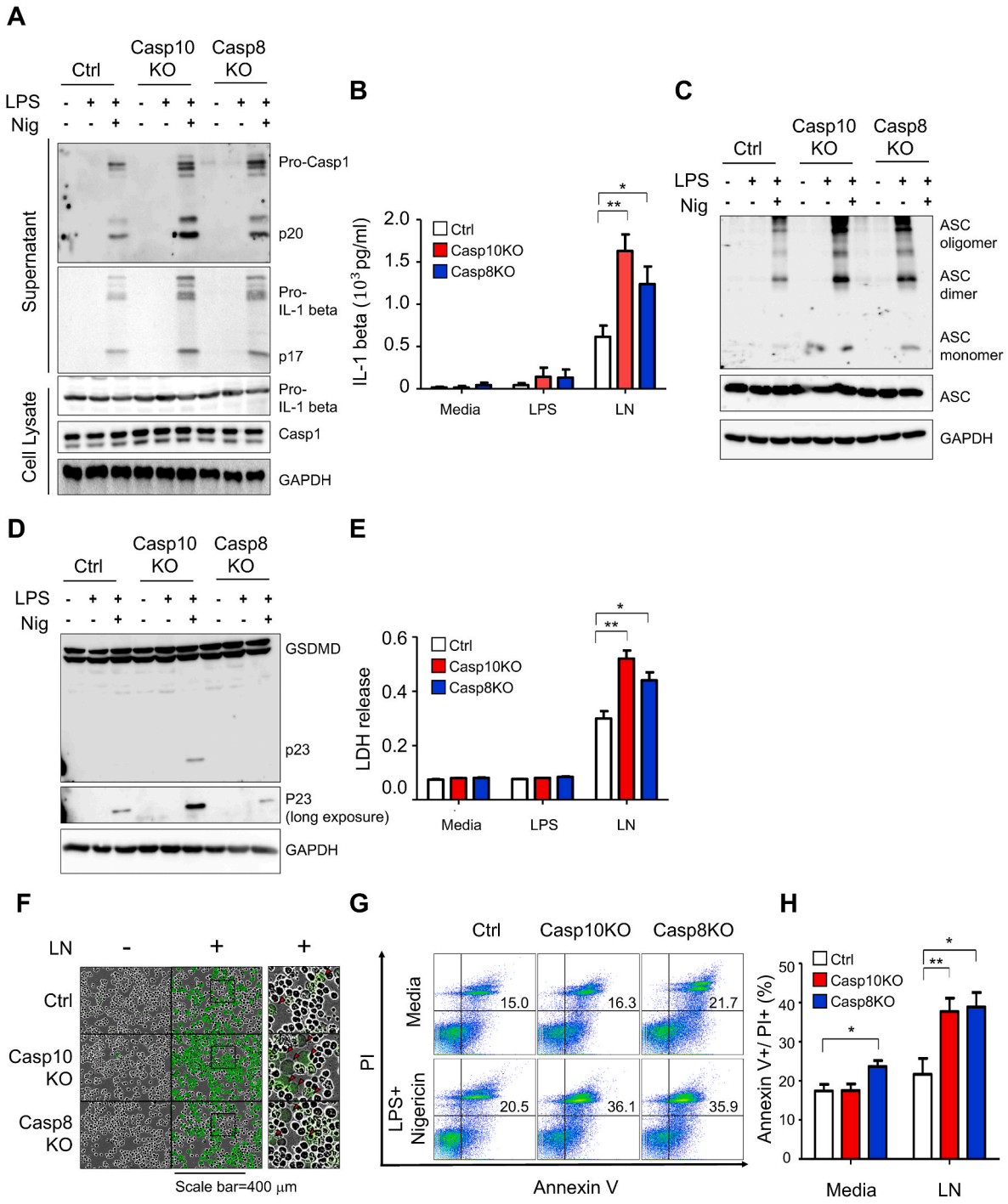

Fig. 4. Caspase-10 inhibits assembly of the NLRP3 inflammasome and pyroptosis in macrophages. (A) Immunoblots for caspase-1, IL-1β, and GAPDH were carried out on supernatant and cell lysate samples. p20 and p17 indicate cleaved fragments of caspase-1 and IL-1β, respectively. Control (Ctrl), caspase-10 knockout (Casp10 KO), and caspase-8 knockout (Casp8 KO) U937 cells were treated with 10 nM PMA overnight. Following that, 1 μg/mL LPS-primed Ctrl, Casp10 KO, and Casp8 KO cells were stimulated with 5 μM nigericin (Nig), for 45 min. (B) ELISA for IL-1β release from the media or from LPS- or LPS + Nig-treated Ctrl, Casp10 KO, and Casp8 KO macrophages (n = 3; *P < 0.05 and **P < 0.01 *vs.* Ctrl, Student's *t*-test). (C) Immunoblots for ASC and GAPDH were carried out in samples from untreated or LPS- or LPS + Nig-treated Ctrl, Casp10 KO, and Casp8 KO macrophages. NLRP3-dependent ASC oligomerization was detected using a disuccinimidyl suberate crosslinker. (D) Immunoblots for GSDMD and GAPDH were carried out on samples from untreated or LPS- or LPS + Nig-treated Ctrl, Casp10 KO, and Casp8 KO macrophages. p23 indicates cleaved GSDMD. (E) LDH release from media or LPS- or LPS + Nig-treated control, Casp10 KO, and Casp8 KO macrophages (n = 3). (F) Representative IncuCyte® images showing pyroptosis in cells treated with LPS and Nig. U937 cells were stained with IncuCyte® Cytotox Green. Right panels show zoomed images of the area marked with squares. Arrowheads indicate pyroptotic cells. (G) Annexin V/PI-stained cell death assay of media or LPS + Nig-treated Ctrl, Casp10 KO, and Casp8 KO macrophages (n = 3).

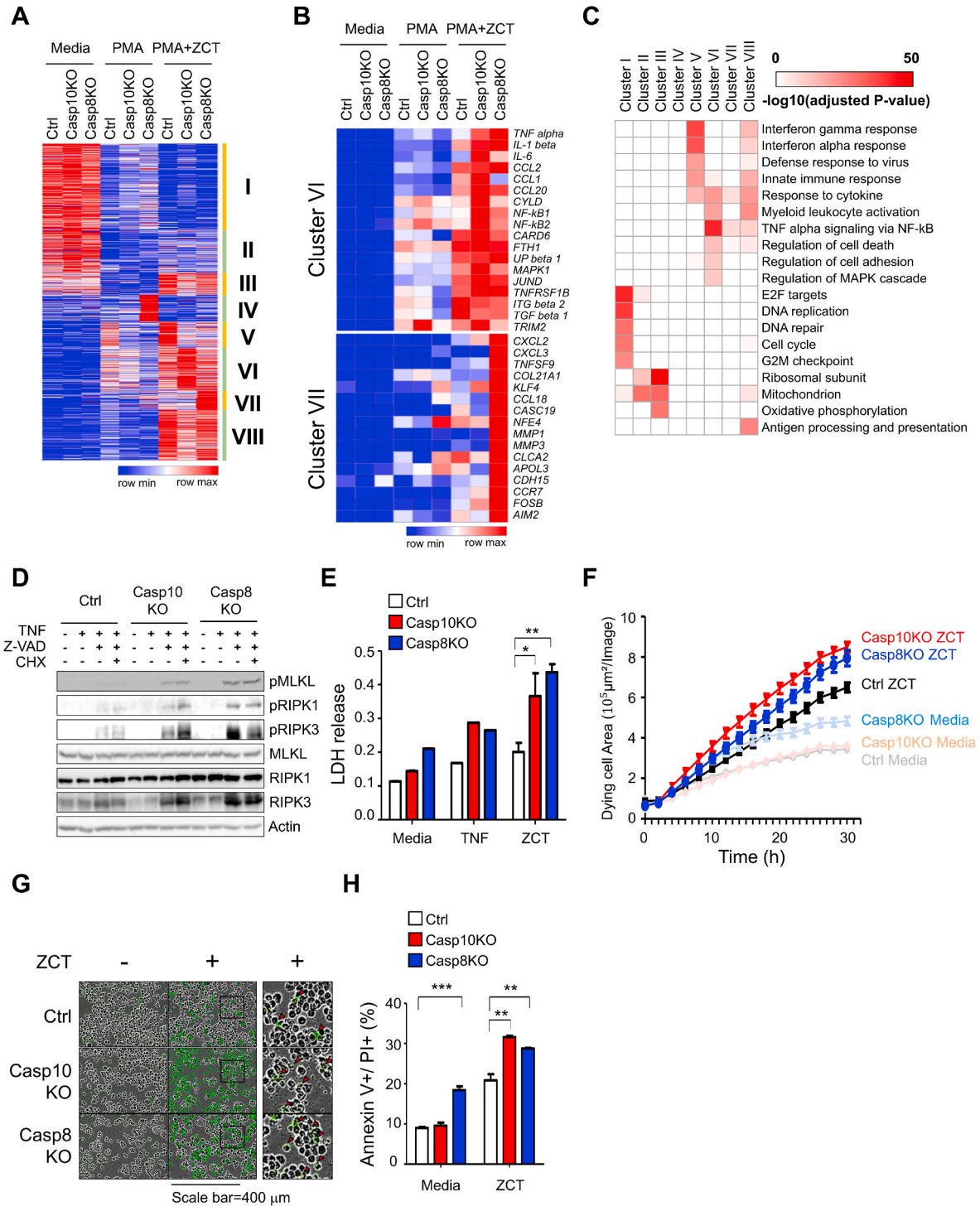

Fig. 5. Caspase-10 inhibits TNF-α-induced necroptosis in macrophages. (A) RNA-seq data analysis using K-means clustering of control (Ctrl), caspase-10 knockout (Casp10 KO), and caspase-8 knockout (Casp8 KO) U937 cells under media-, PMA (10 nM of PMA overnight)-, or PMA + ZCT (10 nM of PMA overnight/20 μM Z-VAD-fmk for 30 min, followed by 20 ng/mL TNF-α and 20 ng/mL cycloheximide for 3 h)-treated conditions. (B) Representative genes of Clusters VI and VII are indicated on the right. (C) Heat-maps of significant Gene Ontology terms in each cluster. (D) Immunoblots for pMLKL, pRIPK1, pRIPK3, MLKL, RIPK1, RIPK3, and β-actin in samples from Ctrl, Casp10 KO, and Casp8 KO macrophages treatment with TNF-α (TNF) or ZCT. (E) LDH release from media- or TNF- or ZCT-treated Ctrl, Casp10 KO, and Casp8 KO macrophages (n = 3; *P < 0.05 and **P < 0.01 *vs.* Ctrl, Student's *t*-test). (F) IncuCyte® cell death assay of media- or ZCT-treated Ctrl, Casp10 KO, and Casp8 KO macrophages (n = 3). (G) Representative IncuCyte® images showing necroptosis in cells treated with ZCT. Right panels show zoomed images of the area marked with squares. Arrowheads indicate necroptotic cells. (H) Annexin V/PI-stained cell death assay of media- or ZCT-treated Ctrl, Casp10 KO, and Casp8 KO macrophages (n = 3; ***P < 0.001 *vs.* Ctrl or Casp8 KO, Student's *t*-test).

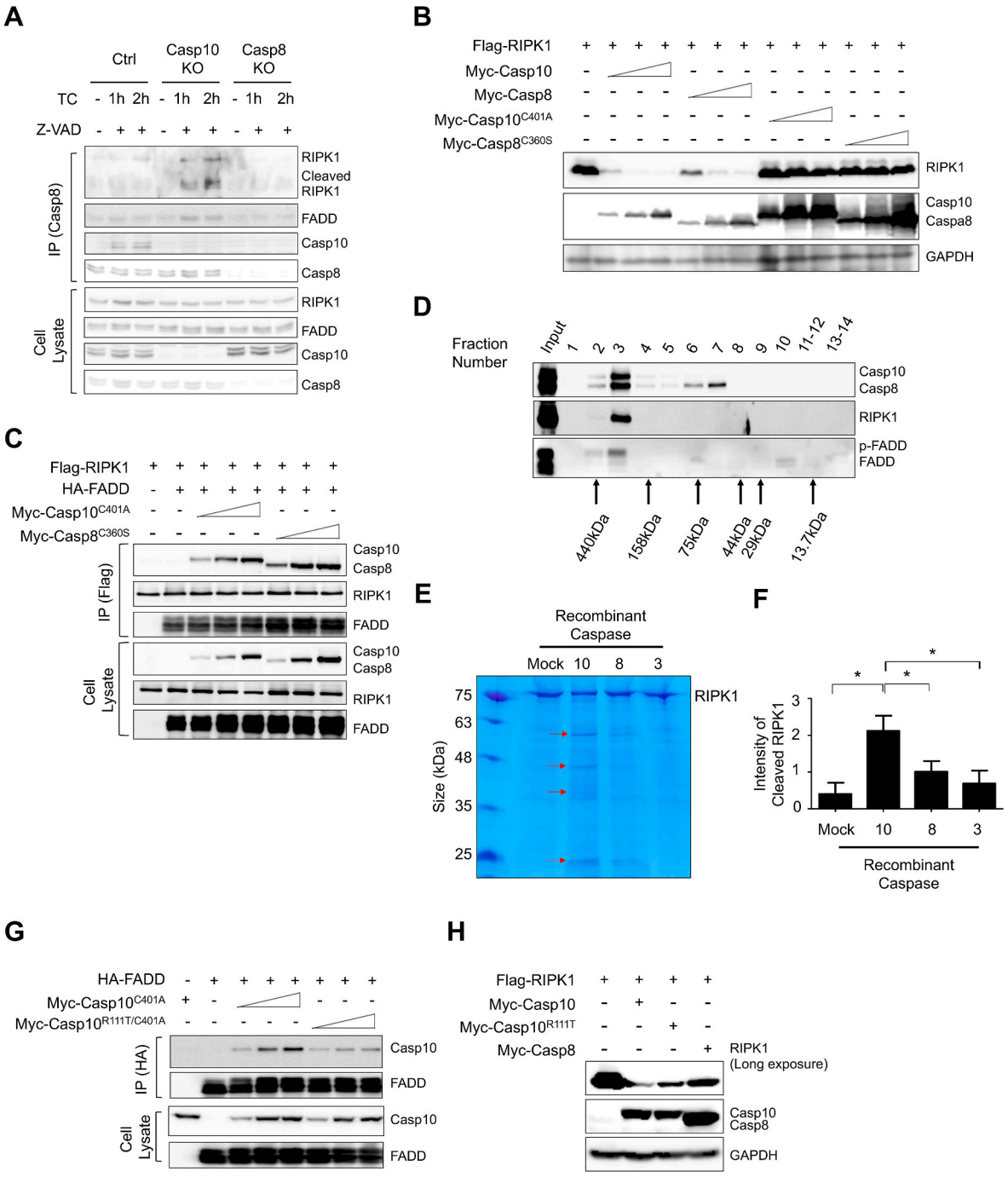

Fig. 6. Both caspase-10 (Casp10) and caspase-8 (Casp8) reduce the necroptosis complex by causing cleavage of RIPK1; however, Casp10 cleaves RIPK1 more actively than Casp8 does, at least under certain circumstances. (A) Immunoblots for endogenous RIPK1, FADD, Casp10, and Casp8 in anti-Casp8 immunoprecipitates [IP (Casp8)] and cell lysates from untreated or ZCT-treated macrophages. (B) Immunoblot for Flag-RIPK1 in Myc-Casp10-, Myc-Casp8-, Myc-Casp10^{C401A}-, or Myc-Casp8^{C360S}-expressing 293T cells. (C) Immunoblot for either Myc-Casp10^{C401A} or Myc-Casp8^{C360S} that were co-immunoprecipitated with Flag-tagged RIPK1 [IP (Flag)]. (D) Gel-filtration assay of 293T cell lysates expressing Myc-Casp10^{C401A}, Myc-Casp8^{C360S}, Flag-RIPK1, and HA-FADD. (E) Coomassie Blue-stained SDS-PAGE gel for assessment of recombinant RIPK1 that was cleaved by active recombinant Casp10, Casp8, or caspase-3. Arrows indicate the cleaved forms of RIPK1. (F) Quantification of the cleaved *N*-terminal fragment of RIPK1 using ImageJ software (n = 3; *P < 0.05 *vs.* Casp10, as assessed using Student's *t*-test). (G) Immunoblot for either Myc-Casp10^{C401A} or Myc-Casp10$^{R111T/C401A}$ in anti-HA-FADD immunoprecipitates [IP (HA)] or cell lysates. (H) Immunoblot for Flag-RIPK1 in Myc-Casp10-, Myc-Casp10^{R111T}-, or Myc-Casp8-expressing 293T cells.

caspase-8.

Finally, we investigated whether the mutation in caspase-10 that was identified in our analysis of patients with PBC also displayed defects in binding with FADD and RIPK1. Caspase-10$^{R111T/C401}$ did not bind with FADD or cleave RIPK1 effectively (Fig. 6G–H).

3.7. Enhanced inflammatory cell death in caspase-10 KO macrophages affects a fibrotic response of HSCs, which can be recovered by treatment with UDCA and OCA

It is well known that inflammatory cells activate HSCs, which is a critical step in the development of liver fibrosis [32]. We hypothesized

that the elevated levels of inflammatory cytokines and enhanced secretion of danger-associated molecular patterns from caspase-10 KO macrophages promote a fibrotic response of HSCs. To prove the same, we collected supernatants from LPS and Nig-treated macrophages, and treated HSCs (LX-2 cells) with the same. Cell migration assay revealed significantly elevated activation in HSCs (by 10.5%; P = 0.012) that were treated with the supernatants of caspase-10 KO macrophages (Supplementary Fig. 8A and B). Moreover, since hepatic fibrosis is a pathological condition that is characterized by extracellular matrix components including matrix metalloproteinase 3, alpha-smooth muscle actin, and transforming growth factor-β1, we checked their expression levels [32], and found that HSCs treated with the supernatants of caspase-10 KO macrophages displayed elevated expression levels of all three (Supplementary Figure 8C). In addition, we observed significantly increased activation in HSCs (by 18.2%; P = 0.006) that were treated with the supernatants of caspase-10 KO macrophages after ZCT induction (Supplementary Fig. 8D–F).

Currently, there are two US Food and Drug Association-approved drugs for the treatment of PBC. One of them is UDCA, a non-cytotoxic and hydrophilic bile acid [33] that has recently been shown to control inflammation through inhibition of the NLRP3 inflammasome [34], while the other is OCA, which is known to have anti-inflammatory and anti-cholestatic effects [35]. Using live-cell death assay, we confirmed that the activation of macrophages is recovered upon treatment with UDCA and OCA (Supplementary Fig. 9A–C).

4. Discussion

Recent GWAS have identified several susceptibility loci, including human leukocyte antigen and non-human leukocyte antigen variants, and provided insights into the genetic architecture of PBC. The identified risk variants highlight that the immunoregulatory pathway contributes to the pathogenesis of PBC. However, the exact genetic mechanism of PBC remains undetermined. This study identified a rare missense variant of *CASP10* by employing WES in samples from a family in which four sisters were diagnosed with PBC. Further, Sanger's sequencing of *CASP10* in 62 additional patients with PBC revealed that there are rare variants that are enriched in sporadic patients with PBC. The rare variant in *CASP10* had a significant association with PBC risk (OR, 9.888; 95% CI, 3.130–31.235; P = 0.002). We generated caspase-10 KO macrophages, which showed elevated expression levels of inflammatory cytokines and more inflammatory cell deaths, upon various immunological stimulations. Thus, our findings suggest that possible dysregulation of cell death and inflammatory responses due to caspase-10 dysfunction might be involved in the pathogenesis of PBC.

Germline loss-of-function mutations in *CASP10* are causative of type IIA autoimmune lymphoproliferative syndrome (ALPS) [36]. ALPS is a rare disease that is characterized by immune dysregulation due to defective lymphocyte homeostasis [36]. The most common genetic cause of ALPS is a pathogenic variant in the Fas cell surface death receptor (*FAS*; a type IA ALPS) gene, while some patients have mutations in other genes relevant for the Fas pathway of apoptosis, such as *CASP10* and Fas ligand (*FASLG*; a type IB ALPS) [36]. Somatic *CASP10* mutations are also associated with non-Hodgkin's lymphoma and gastric cancer [37,38]. Caspase-10 contains two DEDs, which mediate its dimerization and interaction with the DED of FADD and a catalytic protease domain that is further processed into a p17 large and a p12 small subunit [39]. The first reported pathogenic variant (caspase-10^{L285F}) associated with ALPS is located in the p17 large protease-coding region of *CASP10* [40]. The variant showed impaired caspase activity and defects in induction of apoptosis, with a dominant negative effect [40]. The two *CASP10* variants detected in our patients (caspase-10^{R111T} and caspase-10^{L105P}) are located in the linker segment between the two DEDs of caspase-10 (Supplementary Table 1). The caspase-10^{R111T} has been previously identified in a study by Shin et al. on tissue samples from non-Hodgkin's lymphoma patients [37]. The other adjacent variant caspase-10^{V112I} identified in the lymphoma tissue in this study was also located in the same linker segment between the two DEDs [37]. The two linked region missense variants identified in the lymphoma tissue, caspase-10^{R111T} and caspase-10^{V112I}, showed significant impairment of apoptosis, just like that observed in case of variants in the prodomain and protease domains [37]. The authors described that these amino acid changes in a DED linker segment might lead to structural changes in caspase-10 and interfere with the DED-DED interaction between FADD and caspase-10 [37]. Indeed, our structural analysis supports this hypothesis, by showing that the caspase-10^{R111T} variant could affect the tertiary structure of caspase-10, resulting in impaired interaction between caspase-10^{R111T} and FADD. In addition, a missense variant caspase-10^{K99}, which is also located in the linker between the two DEDs, was recently identified in a patient diagnosed with ALPS, using a targeted gene panel [41]. These findings suggest that amino acid changes in the DED linker segment could impair the function of caspase-10, resulting in the pathogeneses of diseases such as PBC, ALPS, and lymphoma.

Caspases are a family of cysteine proteases that hydrolyze their substrates after specific aspartic acid residues [42]. It has been long known that caspases are involved in cell death (initiator apoptotic caspases: caspase-8, -9, and -10; and effector apoptotic caspases: caspase-3, -6, and -7) and inflammation response (caspase-1) [42]. Among all caspases, there are only two that have two DED domains in their *N*-terminus; caspase-8 and caspase-10. Caspase-8 is constitutively and widely expressed in most rodent and human cells, while caspase-10 is expressed in all primates and only a subset of rodents (guinea pigs, but not mice and rats) [42]. Caspase-10 has been believed to serve as an apoptosis initiator, similar to caspase-8; however, there is not much evidence regarding the same. Recently, new types of cell death distinct from apoptosis are attracting attention. In these types of cell death, danger-associated molecular patterns such as HMGB1 are released through pores in cell membranes, which cause inflammatory responses in the neighboring cells. Necroptosis and pyroptosis are representative types of such inflammatory cell deaths [43]. Of note, caspase-8 is a key molecule that determines apoptosis and inflammatory cell death. When caspase-8 is active, it activates caspase-3 to cause apoptosis [44]. Another simultaneous role of caspase-8 is to degrade RIPK1. However, if caspase-8 loses its activity, it cannot degrade RIPK1, which in turn causes phosphorylation of RIPK1, RIPK3, and MLKL, consequently inducing necroptosis [45]. To the best of our knowledge, the roles of caspase-10 in inflammatory cell deaths have not been studied.

In this study, our data suggests that caspase-10 shares the distinct roles of caspase-8 during differentiation into macrophages, upon various immune stimulations. While caspase-8 plays a sensitive role in cell deaths, including necrosis and apoptosis, during differentiation, caspase-10 does not. However, upon immune stimulation in macrophages, caspase-10 regulates the process of inflammatory cell death more strongly than caspase-8, due to its enhanced enzymatic activity to cleave RIPK1, which might also influence inflammasome formation.

5. Conclusion

Our study provided the first comprehensive insight into a novel genetic link between caspase-10 and PBC. We have demonstrated that caspase-10 is a *bona fide* inhibitor of pyroptosis, necroptosis, and pro-inflammatory cytokine production in macrophages. Our findings indicate that the *CASP10* variant-mediated dysregulation of inflammatory response could be involved in PBC pathogenesis. They also indicate that the *CASP10* variant could provide a genetically susceptible environment for both senescence and inflammation, which are important in PBC pathogenesis. Nonetheless, causative variants identified in PBC patient family described in this study may not apply to all PBC patients. Also the role of caspase-10 examined in U937 cell lines may differ from studies in primary cells. It would be better to use clinical samples such as serum and liver macrophages before and after UDCA or OCA treatment. However, further investigation of the related signaling cascades and

downstream targets of the variant gene identified in this study should provide insight into the mechanisms underlying PBC.

Author contributions

M.C. and S·H.D. collected the data, performed the experiments, analyzed the data, and wrote the manuscript. S.S. and K.-A. L. conceived the study, analyzed the data, and wrote the manuscript. Y.L., Y·K., J.L., and S.J.Y. contributed to the data interpretation. S.H.P. conceived the study and analyzed the data. L.K.K. conceived the study, analyzed the data and wrote the manuscript. All authors read and approved the final manuscript.

Declaration of competing interest

The authors disclose no conflicts.

Data availability

Data will be made available on request.

Acknowledgements

We thank all members of Prof. Lark Kyun Kim's lab for helping the experiments and critical reading of the manuscript. This work was supported by the National Research Foundation of Korea (NRF) grant funded by the Korea government (MSIT) (NRF-2021R1A4A5032185).

Appendix A. Supplementary data

Supplementary data to this article can be found online at https://doi.org/10.1016/j.jaut.2022.102940.

References

[1] A.F. Gulamhusein, G.M. Hirschfield, Primary biliary cholangitis: pathogenesis and therapeutic opportunities, Nat. Rev. Gastroenterol. Hepatol. 17 (2020) 93–110.
[2] A.C. Cheung, W.J. Lammers, C.F. Murillo Perez, H.R. van Buuren, A. Gulamhusein, P.J. Trivedi, et al., Effects of age and sex of response to ursodeoxycholic acid and transplant-free survival in patients with primary biliary cholangitis, Clin. Gastroenterol. Hepatol. 17 (2019) 2076–20784 e2.
[3] H. Zhang, M. Carbone, A. Lleo, P. Invernizzi Geoepidemiology, Genetic and environmental risk factors for PBC, Dig. Dis. 33 (Suppl 2) (2015) 94–101.
[4] Z. Shuai, M.W. Leung, X. He, W. Zhang, G. Yang, P.S. Leung, et al., Adaptive immunity in the liver, Cell. Mol. Immunol. 13 (2016) 354–368.
[5] A. Lleo, C.L. Bowlus, G.X. Yang, P. Invernizzi, M. Podda, J. Van de Water, et al., Biliary apotopes and anti-mitochondrial antibodies activate innate immune responses in primary biliary cirrhosis, Hepatology 52 (2010) 987–998.
[6] T.K. Mao, Z.X. Lian, C. Selmi, Y. Ichiki, P. Ashwood, A.A. Ansari, et al., Altered monocyte responses to defined TLR ligands in patients with primary biliary cirrhosis, Hepatology 42 (2005) 802–808.
[7] J.P. Pradere, J. Kluwe, S. De Minicis, J.J. Jiao, G.Y. Gwak, D.H. Dapito, et al., Hepatic macrophages but not dendritic cells contribute to liver fibrosis by promoting the survival of activated hepatic stellate cells in mice, Hepatology 58 (2013) 1461–1473.
[8] I. Bianchi, M. Carbone, A. Lleo, P. Invernizzi, Genetics and epigenetics of primary biliary cirrhosis, Semin. Liver Dis. 34 (2014) 255–264.
[9] A.F. Gulamhusein, B.D. Juran, K.N. Lazaridis, Genome-wide association studies in primary biliary cirrhosis, Semin. Liver Dis. 35 (2015) 392–401.
[10] F. Qiu, R. Tang, X. Zuo, X. Shi, Y. Wei, X. Zheng, et al., A genome-wide association study identifies six novel risk loci for primary biliary cholangitis, Nat. Commun. 8 (2017), 14828.
[11] B. Zhong, P. Strnad, C. Selmi, P. Invernizzi, G.Z. Tao, A. Caleffi, et al., Keratin variants are overrepresented in primary biliary cirrhosis and associate with disease severity, Hepatology 50 (2009) 546–554.
[12] G. Hudson, A. Gomez-Duran, I.J. Wilson, P.F. Chinnery, Recent mitochondrial DNA mutations increase the risk of developing common late-onset human diseases, PLoS Genet. 10 (2014), e1004369.
[13] S. Marzorati, A. Lleo, M. Carbone, M.E. Gershwin, P. Invernizzi, The epigenetics of PBC: the link between genetic susceptibility and environment, Clin Res Hepatol Gastroenterol 40 (2016) 650–659.
[14] D. Weng, R. Marty-Roix, S. Ganesan, M.K. Proulx, G.I. Vladimer, W.J. Kaiser, et al., Caspase-8 and RIP kinases regulate bacteria-induced innate immune responses and cell death, Proc. Natl. Acad. Sci. U. S. A. 111 (2014) 7391–7396.
[15] J. Sarhan, B.C. Liu, H.I. Muendlein, P. Li, R. Nilson, A.Y. Tang, et al., Caspase-8 induces cleavage of gasdermin D to elicit pyroptosis during Yersinia infection, Proc. Natl. Acad. Sci. U. S. A. 115 (2018) E10888–E10897.
[16] K. Wachmann, C. Pop, B.J. van Raam, M. Drag, P.D. Mace, S.J. Snipas, et al., Activation and specificity of human caspase-10, Biochemistry 49 (2010) 8307–8315.
[17] S. Shin, I.H. Moh, Y.S. Woo, S.W. Jung, J.B. Kim, J.W. Park, et al., Evidence from a familial case suggests maternal inheritance of primary biliary cholangitis, World J. Gastroenterol. 23 (2017) 7191–7197.
[18] K. Labun, T.G. Montague, J.A. Gagnon, S.B. Thyme, E. Valen, CHOPCHOP v2: a web tool for the next generation of CRISPR genome engineering, Nucleic Acids Res. 44 (2016) W272–W276.
[19] P. Migliorini, P. Italiani, F. Pratesi, I. Puxeddu, D. Boraschi, The IL-1 family cytokines and receptors in autoimmune diseases, Autoimmun. Rev. 19 (2020), 102617.
[20] C.A. Yang, B.L. Chiang, Inflammasomes and human autoimmunity: a comprehensive review, J. Autoimmun. 61 (2015) 1–8.
[21] V. Barak, C. Selmi, M. Schlesinger, M. Blank, N. Agmon-Levin, I. Kalickman, et al., Serum inflammatory cytokines, complement components, and soluble interleukin 2 receptor in primary biliary cirrhosis, J. Autoimmun. 33 (2009) 178–182.
[22] M.P. Stoppelli, A. Corti, A. Soffientini, G. Cassani, F. Blasi, R.K. Assoian, Differentiation-enhanced binding of the amino-terminal fragment of human urokinase plasminogen activator to a specific receptor on U937 monocytes, Proc. Natl. Acad. Sci. U. S. A. 82 (1985) 4939–4943.
[23] H. Guan, L. Xie, F. Leithauser, L. Flossbach, P. Moller, T. Wirth, et al., KLF4 is a tumor suppressor in B-cell non-Hodgkin lymphoma and in classic Hodgkin lymphoma, Blood 116 (2010) 1469–1478.
[24] A. Kumar, S. Tikoo, S. Maity, S. Sengupta, S. Sengupta, A. Kaur, et al., Mammalian proapoptotic factor ChaC1 and its homologues function as gamma-glutamyl cyclotransferases acting specifically on glutathione, EMBO Rep. 13 (2012) 1095–1101.
[25] X. Liu, Z. Zhang, J. Ruan, Y. Pan, V.G. Magupalli, H. Wu, et al., Inflammasome-activated gasdermin D causes pyroptosis by forming membrane pores, Nature 535 (2016) 153–158.
[26] M. Fritsch, S.D. Gunther, R. Schwarzer, M.C. Albert, F. Schorn, J.P. Werthenbach, et al., Caspase-8 is the molecular switch for apoptosis, necroptosis and pyroptosis, Nature 575 (2019) 683–687.
[27] S. Grootjans, T. Vanden Berghe, P. Vandenabeele, Initiation and execution mechanisms of necroptosis: an overview, Cell Death Differ. 24 (2017) 1184–1195.
[28] R. Kumari, R.S. Deshmukh, S. Das, Caspase-10 inhibits ATP-citrate lyase-mediated metabolic and epigenetic reprogramming to suppress tumorigenesis, Nat. Commun. 10 (2019) 4255.
[29] Y. Imai, T. Kimura, A. Murakami, N. Yajima, K. Sakamaki, S. Yonehara, The CED-4-homologous protein FLASH is involved in Fas-mediated activation of caspase-8 during apoptosis, Nature 398 (1999) 777–785.
[30] K.M. Boatright, M. Renatus, F.L. Scott, S. Sperandio, H. Shin, I.M. Pedersen, et al., A unified model for apical caspase activation, Mol. Cell. 11 (2003) 529–541.
[31] L. Zhang, K. Blackwell, L.M. Workman, S. Chen, M.R. Pope, S. Janz, et al., RIP1 cleavage in the kinase domain regulates TRAIL-induced NF-kappaB activation and lymphoma survival, Mol. Cell Biol. 35 (2015) 3324–3338.
[32] A. Woodhoo, M. Iruarrizaga-Lejarreta, N. Beraza, J.L. Garcia-Rodriguez, N. Embade, D. Fernandez-Ramos, et al., Human antigen R contributes to hepatic stellate cell activation and liver fibrosis, Hepatology 56 (2012) 1870–1882.
[33] R.E. Poupon, B. Balkau, E. Eschwege, R. Poupon, A multicenter, controlled trial of ursodiol for the treatment of primary biliary cirrhosis. UDCA-PBC Study Group, N. Engl. J. Med. 324 (1991) 1548–1554.
[34] C. Guo, S. Xie, Z. Chi, J. Zhang, Y. Liu, L. Zhang, et al., Bile acids control inflammation and metabolic disorder through inhibition of NLRP3 inflammasome, Immunity 45 (2016) 802–816.
[35] S. Mudaliar, R.R. Henry, A.J. Sanyal, L. Morrow, H.U. Marschall, M. Kipnes, et al., Efficacy and safety of the farnesoid X receptor agonist obeticholic acid in patients with type 2 diabetes and nonalcoholic fatty liver disease, Gastroenterology 145 (2013) 574–582 e1.
[36] P. Li, P. Huang, Y. Yang, M. Hao, H. Peng, F. Li, Updated understanding of autoimmune lymphoproliferative syndrome (ALPS), Clin. Rev. Allergy Immunol. 50 (2016) 55–63.
[37] M.S. Shin, H.S. Kim, C.S. Kang, W.S. Park, S.Y. Kim, S.N. Lee, et al., Inactivating mutations of CASP10 gene in non-Hodgkin lymphomas, Blood 99 (2002) 4094–4099.
[38] W.S. Park, J.H. Lee, M.S. Shin, J.Y. Park, H.S. Kim, J.H. Lee, et al., Inactivating mutations of the caspase-10 gene in gastric cancer, Oncogene 21 (2002) 2919–2925.
[39] P. Fuentes-Prior, G.S. Salvesen, The protein structures that shape caspase activity, specificity, activation and inhibition, Biochem. J. 384 (2004) 201–232.
[40] J. Wang, L. Zheng, A. Lobito, F.K. Chan, J. Dale, M. Sneller, et al., Inherited human Caspase 10 mutations underlie defective lymphocyte and dendritic cell apoptosis in autoimmune lymphoproliferative syndrome type II, Cell 98 (1999) 47–58.
[41] E. Omoyinmi, A. Standing, A. Keylock, F. Price-Kuehne, S. Melo Gomes, D. Rowczenio, et al., Clinical impact of a targeted next-generation sequencing gene panel for autoinflammation and vasculitis, PLoS One 12 (2017), e0181874.
[42] N. Van Opdenbosch, M. Lamkanfi, Caspases in cell death, inflammation, and disease, Immunity 50 (2019) 1352–1364.

[43] R. Schwarzer, L. Laurien, M. Pasparakis, New insights into the regulation of apoptosis, necroptosis, and pyroptosis by receptor interacting protein kinase 1 and caspase-8, Curr. Opin. Cell Biol. 63 (2020) 186–193.
[44] H.R. Stennicke, J.M. Jurgensmeier, H. Shin, Q. Deveraux, B.B. Wolf, X. Yang, et al., Pro-caspase-3 is a major physiologic target of caspase-8, J. Biol. Chem. 273 (1998) 27084–27090.
[45] K. Newton, K.E. Wickliffe, D.L. Dugger, A. Maltzman, M. Roose-Girma, M. Dohse, et al., Cleavage of RIPK1 by caspase-8 is crucial for limiting apoptosis and necroptosis, Nature 574 (2019) 428–431.